Received: 6 February 2016 | Revised: 27 April 2016 | Accepted: 2 July 2016

DOI 10.1002/aoc.3577

WILEY Applied Organometallic Chemistry

FULL PAPER

DNA interaction, antimicrobial and molecular docking studies of biologically interesting Schiff base complexes incorporating 4-formyl-*N*,*N*-dimethylaniline and propylenediamine

Seemon Packianathan | Ganesan Kumaravel | Natarajan Raman*

Research Department of Chemistry, VHNSN College, Virudhunagar 626 001, Tamilnadu, India

Correspondence
Natarajan Raman, Research Department of Chemistry, VHNSN College, Virudhunagar – 626 001, India.
E-mail: ramchem1964@gmail.com

Four new transition metal complexes incorporating a Schiff base ligand derived from propylenediamine and 4-formyl-*N*,*N*-dimethylaniline have been synthesized using transition metal salts. The characterization of the newly formed complexes was done from physicochemical parameters and using various techniques like ^{1}H NMR, ^{13}C NMR, IR, UV, electron paramagnetic resonance and mass spectroscopies, powder X-ray diffraction and magnetic susceptibility. All the complexes were found to be monomeric in nature with square planar geometry. X-ray powder diffraction illustrates that the complexes have a crystalline nature. The interaction of metal complexes with calf thymus DNA was investigated using UV–visible absorption, viscosity measurements, cyclic voltammetry, emission spectroscopy and docking analysis. The results indicate that the Cu(II), Co(II), Ni(II) and Zn(II) complexes interact with DNA by intercalative binding mode with optimum intrinsic binding constants of 4.3×10^4, 3.9×10^4, 4.7×10^4 and 3.7×10^4 M^{-1}, respectively. These DNA binding results were rationalized using molecular docking in which the docked structures indicate that the metal complexes fit well into the A-T rich region of target DNA through intercalation. The metal complexes exhibit an effective cleavage with pUC19 DNA by an oxidative cleavage mechanism. The synthesized ligand and the complexes were tested for their *in vitro* antimicrobial activity. The complexes show enhanced antifungal and antibacterial activities compared to the free ligand.

KEYWORDS

antimicrobial study, DNA binding, molecular docking analysis, propylenediamine

1 | INTRODUCTION

Schiff bases are an important class of inorganic and organic compounds with a variety of uses. They have been widely engaged as ligands in the formation of transition metal complexes.[1,2] Schiff bases containing heterocyclic moieties possess more interesting properties due to their diverse anticancer, antiviral, fungicidal, bactericidal, anti-inflammatory and anti-HIV activities.[3,4] Thus, the development of new chemotherapeutic Schiff bases is now attracting the attention of medicinal chemists.[5] The chemistry of Schiff base compounds as well as their metal complexes is of great interest in various fields of chemical and biological research.[6] They are also very useful model systems in chelate chemistry. The metal ion of the complexes can be coordinated by the imine nitrogen atom and also other active centres present in the molecule. These can be lead to many interesting catalytic and other potential properties.[7–9] In recent decades, metallocomplexes have attracted much attention in chemistry, biochemistry and pharmacology as hopeful compounds for the creation of novel drugs. Propylenediamine derivatives of the type [$PtCl_2$(*N*-benzyl-1,3-propanediamine)$_2$] have been reported as potential antitumor agents.

Antimicrobial and DNA-binding studies are very important in the development and advancement of new therapeutic

reagents and DNA molecular probes.[10–12] Recently, there has been tremendous interest in studies associated with the interaction of transition metal ions with nucleic acids and the important development of new reagents for biotechnology and medicine.[13] Metal complexes with their variable coordination environment and adaptable redox and spectral properties have been proposed for designing species that are suitable to bind to and cleave DNA.[14] Small molecules can interact with DNA through the following three non-covalent modes: intercalation, groove binding and external electrostatic effects. Among these interactions, intercalation is one of the most important DNA-binding modes, which is related to the antitumor activity of a compound. Small metal complexes undergo hydrolytic DNA cleavage which is very useful in genetic engineering molecular biotechnology and robust anticancer drug design.[15,16] Recently, there has been a great interest in the binding of metal complexes with DNA[17–23] because it may provide important information for new cancer therapeutic agents and potential probes of DNA structure and conformation. Hence, much attention has been targeted on the design of metal-based complexes, particularly transition metal complexes which can bind to and cleave DNA effectively.

It is our aim to design an appropriate ligand to obtain the optimum metal complex to resolve the challenges that have arisen earlier. Thus, encouraged by the advancements discussed above, herein we report our newly synthesized Schiff base transition metal complexes derived from a bidentate Schiff base ligand (using 4-formyl-*N*,*N*-dimethylaniline and propane-1,3-diamine) together with their characterization by employing the techniques of Fourier transform infrared (FT-IR), UV–visible and electron paramagnetic resonance (EPR) spectroscopies, ESI-MS and powder X-ray diffraction. Furthermore, interaction of the metal (II) complexes with DNA was also studied to get additional features of their binding modes. Also, the bioactivity of these complexes was assayed for Gram-positive, Gram-negative and fungal strains.

2 | EXPERIMENTAL

2.1 | Materials and methods

All chemicals used were of analytical reagent grade. 4-Formyl-*N*,*N*-dimethylaniline, propylenediamine, calf thymus (CT) DNA, pUC19 DNA and ethidium bromide (EB) were obtained from Sigma Aldrich. All metal salts were obtained from E-Merck and used without further purification. Solvents dimethylformamide and dimethylsulfoxide (DMSO) and agar were procured from Hi-media Chemicals. The solvents were purified by following the standard procedures.[24]

Elemental analysis (C, H and N) data were obtained using a PerkinElmer 240 elemental analyser. Electronic spectra of the complexes were recorded with a Shimadzu model 1601 UV–visible spectrophotometer in the wavelength range 200–1100 nm. FT-IR spectra were recorded with a Shimadzu model IR-Affinity-1 spectrophotometer using KBr pellets in the range 350–4000 cm^{-1}. Proton NMR spectra of the ligand and the complexes were recorded with a Bruker Avance DRX 300 FT-NMR spectrometer using tetramethylsilane as the internal standard. Room temperature magnetic susceptibility measurements were carried out with a modified Gouy-type magnetic balance (Hertz SG8-5HJ). The room temperature molar conductivity of the complexes in DMSO solution (10^{-3} M) was measured using a Deep Vision 601 digital conductometer. The X-band EPR spectra were obtained at liquid nitrogen temperature (77 K) using tetracyanoethylene as the g-marker. Redox properties of complexes were determined with a CHI 620C electrochemical analyser. The measurements were carried out under nitrogen atmosphere using a three-electrode cell in which a glassy carbon, saturated Ag/AgCl and platinum wire were used as the working, reference and auxiliary electrodes, respectively. Powder X-ray diffraction patterns were recorded with an X'Pert PRO diffractometer using Cu $K\alpha_1$ radiation (λ = 1.54060 Å) with an operating voltage of 40 kV and a current of 30 mA. All fluorescence emission measurements were performed with a JASCO spectrofluorimeter (FP6200) using a quartz cuvette of 1 cm path length.

2.2 | Preparation of Schiff base ligand (L)

Synthesis of the Schiff base was done by the dropwise addition of an ethanolic solution of 4-formyl-*N*,*N*-dimethylaniline (0.02 M) to an ethanolic solution of propylenediamine (0.01 M). The reaction mixture was refluxed for 3 h. A pale yellow coloured solution was obtained. Then the solution was reduced to one-third using a water bath. The precipitated solid complex was filtered off, washed thoroughly with ethanol and dried in *vacuo*. The yield was 77%. The analytical and physical data of the Schiff base ligand and its complexes are given in the supporting information (Table S1).

[$C_{21}H_{28}N_4$]. Yield 82%. Anal. Calcd (%): C, 74.96; H, 8.39; N, 16.65. Found (%): C, 74.48; H, 8.18; N, 16.48). FT-IR (KBr, cm^{-1}): 1610 ν(HC═N), 1220–1260 ν(C─N─C), 2900–2950 ν(C─H), 1400–1600 ν(C═C). ^{1}H NMR (DMSO-d_6, δ, ppm): 6.8–7.5 (m, aromatic), 3.7 (N─CH_2), 2.0 (CH_2), 3.1 (N─CH_3), 8.7 (HC═N). ^{13}C NMR (DMSO-d_6, δ, ppm): 41.3 (C_1), 153.4, 111.9, 124.6, 152.0 (C_2-C_5), 160.8 (C_6), 53.4 (C_7), 32.2 (C_8). UV–visible (DMSO, cm^{-1} (transition)): 27 548 (π–π*), 38 759 (n–π*).

2.3 | Preparation of Schiff base metal complexes

An ethanolic solution of 0.001 M metal(II) chloride was mixed with Schiff base ligand (0.001 M) and the resultant mixture was stirred for 2 h. The reaction mixture was refluxed for 3 h and then the solvent was evaporated under

reduced pressure. The precipitated complexes were isolated and washed with distilled water. They were recrystallized from ethanol and dried in vacuum at room temperature.

[$CuLCl_2$]. Yield: 74%. Anal. Calcd for $C_{21}H_{28}N_4Cl_2Cu$ (%): C, 53.56; H, 5.99; N, 11.90; Cu, 13.49. Found (%): C, 53.18; H, 5.74; N, 11.82; Cu, 13.17. FT-IR (KBr, cm^{-1}): 1571 ν(HC═N), 438 ν(M─N). Λ_m (Ω^{-1} mol^{-1} cm^2): 18.09. μ_{eff} (BM): 1.94. UV–visible (DMSO, cm^{-1} (transition)): 21 186 (d–d).

[$NiLCl_2$]. Yield: 71%. Anal. Calcd for $C_{21}H_{28}N_4Cl_2Ni$ (%): C, 54.12; H, 6.06; N, 12.02; Ni, 12.59. Found (%): C, 54.01; H, 5.91; N, 11.88; Ni, 12.41. FT-IR (KBr, cm^{-1}): 1604 ν(HC═N), 427 ν(M─N). Λ_m (Ω^{-1} mol^{-1} cm^2): 12.57. μ_{eff} (BM): diamagnetic. UV–visible (DMSO, cm^{-1} (transition)): 14 727 (d–d).

[$CoLCl_2$]. Yield: 73%. Anal. Calcd for $C_{21}H_{28}N_4Cl_2Co$ (%): C, 54.09; H, 6.05; N, 12.01; Co, 12.64. Found (%): C, 53.93; H, 5.92; N, 11.92; Co, 12.47. FT-IR (KBr, cm^{-1}): 1598 ν(HC═N), 445 ν(M─N). Λ_m (Ω^{-1} mol^{-1} cm^2): 13.83. μ_{eff} (BM): 3.42. UV–visible (DMSO, cm^{-1} (transition)): 13 793, 12 642 (d–d).

[$ZnLCl_2$]. Yield: 68%. Anal. Calcd for $C_{21}H_{28}N_4Cl_2Zn$ (%): C, 53.35; H, 5.97; N, 11.85; Zn, 13.83. Found (%): C, 53.18; H, 5.82; N, 11.72; Zn, 13.65. FT-IR (KBr, cm^{-1}): 1597 ν(HC═N), 449 ν(M─N). ^{1}H NMR (DMSO-d_6, δ, ppm): 6.8–7.5 (phenyl multiplet), 3.6 (N─CH_2), 2.0 (CH_2), 3.1 (N─CH_3), 8.9 (HC═N). ^{13}C NMR (DMSO-d_6, δ, ppm): 41.3 (C_1), 153.4, 111.9, 124.6, 152.0 (C_2-C_5), 162.3 (C_6), 53.8 (C_7), 32.2 (C_8). Λ_m (Ω^{-1} mol^{-1} cm^2): 14.96. μ_{eff} (BM): diamagnetic.

2.4 | DNA binding assay

To carry out the DNA binding experiment using absorption spectral titrations, an array of solutions was prepared in which the concentration of the complex was maintained constant (0.1 mM) while the concentration of stock CT DNA was increased from solution to solution. The absorption spectra of these different metal complex–DNA solutions were obtained in the range 200–1100 nm. By measuring the alterations in the ligand-to-metal charge transfer absorption band upon increasing DNA concentration, the intrinsic binding constants K_b were calculated. For such calculations, equation (1) was employed by monitoring the changes of absorption in the metal-to-ligand charge transfer band with increasing concentration of DNA:

$$\frac{[DNA]}{\varepsilon_a-\varepsilon_f}=\frac{[DNA]}{\varepsilon_b-\varepsilon_f}+\frac{1}{[K_b(\varepsilon_b-\varepsilon_f)]} \quad (1)$$

In the above equation, [DNA] denotes the concentration of DNA and absorption coefficients ε_a, ε_f and ε_b correspond to A_{obs}/[complex], free complex extinction coefficient and the extinction coefficient of the complex in the totally bound form, respectively. From equation (1), slope $1/(\varepsilon_b - \varepsilon_f)$ and intercept $1/K_b(\varepsilon_b - \varepsilon_f)$ were determined. Finally by comparing the identified slope and intercept, K_b was calculated.

2.5 | UV–visible spectroscopy

Absorption titration experiments were carried out by varying the DNA concentration and maintaining the complex concentration constant. Absorbance values were recorded after each successive addition of DNA solution and equilibration (*ca* 10 min). The absorption data were analysed for an evaluation of the intrinsic binding constant K_b using a reported procedure.[25]

2.6 | Cyclic voltammetry

Electrochemical studies were carried out using a CHI electrochemical analyser, controlled by CHI620C software. Cyclic voltammetry measurements were performed using a glassy carbon working electrode and an Ag/AgCl reference electrode and the supporting electrolyte was 50 mM NaCl, 5 mM Tris buffer (pH = 7.2). All solutions were deoxygenated by purging with nitrogen for 30 min prior to measurements. The degree of reversibility of one-electron transfer reaction can be obtained from the difference between forward and backward peak potentials. The ratio of equilibrium constants for the binding of oxidative and reductive ions to DNA was calculated using the Nernst equation:

$$E_b^0-E_f^0=0.0591\times\log\left(\frac{K_{red}}{K_{ox}}\right) \quad (2)$$

where E_b^0 and E_f^0 are the potentials of the bound and free complex forms, respectively, K_{red} is the binding constant for the binding of reductive ion species with CT DNA and K_{ox} is the binding constant for the binding of oxidative ion species with CT DNA.

2.7 | Viscosity study

Viscosity measurements at room temperature were carried out using a semi-microdilution capillary viscometer. Each experiment was performed three times and an average flow time was calculated. Data were presented as (η/η_0) versus binding ratio, where η is the viscosity of DNA in the presence of complex and η_0 is the viscosity of DNA alone.

2.8 | DNA cleavage

For a solution of pUC19 DNA in buffer (50 mM NaCl/5 mM Tris–HCl; pH = 7.2), the ratio between the UV absorbance at 260 and 280 nm (A_{260}/A_{280}) was 1.89. This suggested that the chosen DNA was sufficiently free of proteins. To accomplish cleavage reactions, solutions of pUC19 DNA were prepared and then diluted with loading dye using 1% agarose

gel. To each solution obtained, 3 µl of EB (0.5 µg ml^{-1}) was added and mixed well. In the next step, warm agarose was poured and instantly held tightly with a comb to develop sample wells. The gel was placed in an electrophoretic tank and adequate electrophoretic buffers were added to enclose the gel to 1 mm depth. DNA sample (20 µM), 30 µM complex and 10 µM H_2O_2 in the aforesaid buffer (pH = 7.2) were mixed with a loading dye and filled into the well of the submerged gel using a micropipette. A 50 mA electric current was passed and the gel was taken out from the buffer. The gel was photographically captured under UV light after the completion of electrophoresis.

2.9 | Antimicrobial activity

Antibacterial and antifungal activities of the ligand and the synthesized metal complexes were tested *in vitro* against the bacterial species *K. pneumoniae*, *B. subtilis*, *E. coli* and *S. typhi* and the fungi *A. flavus*, *C. albicans* and *A. niger* using the paper disc method with nutrient agar as the medium. Ampicillin was used as the standard antibacterial agent and ciprofloxacin was used as the standard antifungal agent. The test organisms were grown on nutrient agar medium in Petri plates. Discs were prepared and applied over the long culture. The compounds were prepared in DMSO and soaked in filter paper disc of 5 mm in diameter and 1 mm in thickness. The concentrations of ligand and the complexes used in this study were 0.01 µg ml^{-1}. The discs were placed on previously seeded plates and incubated at 37°C and the diameter of the inhibition zone around each disc was measured after 24 h for antibacterial activity and after 74 h for antifungal activity. Growth inhibition was calculated according to the literature.[26]

3 | RESULTS AND DISCUSSION

The synthesized Schiff base ligand and the metal complexes were found to be air-stable at room temperature. The Schiff base ligand was soluble in methanol. The Schiff base metal complexes were insoluble in water, alcohol and chloroform but soluble in DMSO. The molar conductivities (10^{-3} M) of their solutions at room temperature were measured. The lower conductance values of all the complexes in DMSO showed that the chloride ions were present inside of the coordination sphere which was confirmed by silver nitrate test. Moreover, the lower molar conductance of these complexes supported the non-electrolytic nature of the metal complexes. The results of elemental analysis of the metal complexes were in good agreement with the calculated values of molecular formula [$MLCl_2$], where M = metal (II) and L = Schiff base ligand. The synthetic route to the Schiff base ligand and its metal complexes is shown in Scheme 1.

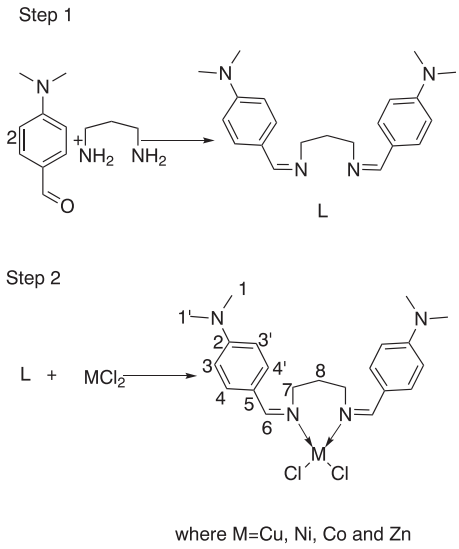

SCHEME 1 Schematic route for synthesis of metal complexes

3.1 | FT-IR spectra

FT-IR spectra afford important information regarding the coordinating sites of a ligand. The FT-IR spectra of the complexes were compared with that of the free ligand to determine the changes that might have taken place during the complexation. The ligand exhibited a band at 1610 cm^{-1} which is assigned to the azomethine nitrogen. In the free ligand spectrum the absorption band measured at 1220–1260 cm^{-1} is attributed to the C—N—C stretching vibration of the $N(CH_3)_2$ moiety.[27] The stretching vibration band appearing at 1610 cm^{-1} for the azomethine group of free ligand is shifted to lower frequency (1571 cm^{-1} in Cu(II); 1604 cm^{-1} in Ni(II); 1598 cm^{-1} in Co(II); 1597 cm^{-1} in Zn (II)) in the spectra of metal complexes, indicating that the azomethine nitrogen is coordinated to the central metal ion in all the complexes. The spectra are shown in Fig. S1. These observed results clearly indicate that the coordination of the Schiff base ligand to the metal centre has occurred as proposed in the presented structure. Generally, for benzene and its derivatives, the aromatic C—H in-plane bending modes are observed in the region 1100–1300 cm^{-1}. For Cu(II), Ni (II), Co(II) and Zn(II) complexes, these FT-IR bands are observed at 1122, 1165, 1232 and 1240 cm^{-1}, respectively. The bands arising from ring C—H out-of-plane bending vibrations are usually observed in the region 650–1000 cm^{-1} for complexes. The bands observed at 939, 812, 727 and 671 cm^{-1} are assigned to ring C—H out-of-plane bending vibrations for the Cu(II), Ni(II), Co(II) and Zn(II) complexes, respectively. Moreover, the formation of complexes is also revealed by the presence of medium intensity (M—N) bands at *ca* 420–450 cm^{-1} which are not observed for the free ligand.[28] The M—Cl stretching bands appearing in the region below 400 cm^{-1} further confirm the complex formation.[29] In conclusion, these data suggest the *N*,*N*-bidentate behaviour of the ligand.

3.2 | Electronic spectra of metal(II) chelates

Electronic spectra of the Schiff base ligand and its metal complexes were recorded in DMSO and are shown in Fig. S2. The electronic absorption spectrum of the Schiff base ligand displayed high-energy bands at 363 nm (27 548 cm^{-1}) and 258 nm (38 759 cm^{-1}), corresponding to $\pi \rightarrow \pi^*$ transition of the aromatic ring and $n \rightarrow \pi^*$ transition of C═N groups, respectively. However, these bands were shifted to 352 nm (28 409 cm^{-1}) and 246 nm (40 650 cm^{-1}) in the spectra of the complexes. The Cu(II) complex displayed a low-intensity broad band at *ca* 472 nm (21 186 cm^{-1}) in the visible region attributed to d–d ($^2B_{1g} \rightarrow {}^2A_{1g}$) transition and suggesting a square planar environment.[30] This geometry is further supported by its magnetic susceptibility value (1.94 BM). On the other hand, the Ni(II) complex showed a lowest energy band appearing at 679 nm (14 727 cm^{-1}) due to d–d ($^1A_{1g} \rightarrow {}^1A_{2g}$) transition as a result of its square planar environment.[31] The electronic spectrum of the Co(II) complex exhibits absorptions at 725 nm (13 793 cm^{-1}) and 791 nm (12 642 cm^{-1}) which are assigned to $^4T_{1g}$ (F) → $^4A_{2g}$(F) and $^4A_{2g}$(F) → $^4T_{1g}$(F) transitions, respectively, corresponding to a Co(II) square planar complex. The geometry is further supported by its magnetic susceptibility value (3.42 BM). In contrast, the Zn(II) complex does not exhibit any d–d band because of its completely filled d^{10} electronic configuration.

3.3 | NMR spectra

The ^{1}H NMR spectra of the Schiff base ligand and the Zn(II) complex were recorded in DMSO-d_6 solution using tetramethysilane as an internal standard. The aromatic proton signals appeared in the region 6.8–7.5 ppm. Schiff base is supported by the presence of azomethine (HC═N) proton signal appearing at 8.7 ppm and a singlet peak at 3.1 ppm for (N─CH_3) protons. The ^{1}H NMR spectrum of the zinc complex shows a singlet peak at 8.9 ppm (CH═N), multiplet peaks at 6.8–7.5 ppm for the aromatic ring protons and a singlet peak at 3.1 ppm for (N─CH_3) protons. From these observations, it is inferred that only the azomethine group (CH═N) is involved in metal coordination. The ^{13}C NMR spectrum of the ligand showed signals of an aromatic carbon at 111.9–153.4 ppm, N─CH_3 carbon at 41.3 ppm, N─CH_2 carbon at 53.8 ppm and CH_2─CH_2 carbon at 32.2 ppm. Moreover, the signal of the (HC═N) carbon at 160.8 ppm for the ligand was shifted to 162.3 ppm upon coordination, indicating that the (HC═N) group participates in complex formation.

3.4 | Mass spectra

Mass spectra provide crucial evidence for elucidating the structure of compounds. The ESI mass spectra of the ligand and its copper complex were recorded to evaluate the stoichiometric composition. The spectrum of the Schiff base showed a molecular ion peak at *m/z* 335 corresponding to $[C_{21}H_{28}N_4]^+$ ion. Also, the spectrum exhibited fragments at *m/z* 120, 147, 161 and 175 corresponding to $[C_8H_{10}N]^+$, $[C_9H_{11}N_2]^+$, $[C_{10}H_{13}N_2]^+$ and $[C_{11}H_{15}N_2]^+$, respectively. The mass spectrum of the Cu(II) complex showed peaks at *m/z* 468, 433, 399, 335 and 131 corresponding to $[C_{21}H_{28}N_4CuCl_2]^+$, $[C_{21}H_{28}N_4CuCl]^+$, $[C_{21}H_{28}N_4Cu]^+$ $[C_{21}H_{28}N_4]^+$ and $[CuCl_2]$, respectively. The mass spectra of the ligand and Cu(II) complex are shown in Figure 1. All the complexes underwent demetallation to form the species $[L]^+$ and provided fragment ion peak at *m/z* 335 which corresponds to the molecular weight of the Schiff base under investigation.

3.5 | Powder X-ray diffraction

We tried to isolate single crystals of the metal complexes for accurate X-ray crystal study but could not succeed in developing single crystals; this might be because of the powder or polycrystalline nature of complexes. Structural information for most inorganic metal complexes is not available because of the powder or polycrystalline nature of these materials. Generally, it is difficult to grow good-quality single crystals of these inorganic complexes. In such cases, powder X-ray diffraction studies might be useful. The X-ray diffraction patterns of the metal complex are shown in Fig. S3 which exhibit reflecting peaks of 2θ scattering angles at 13.55°, 17.29°, 18.54°, 20.04°, 20.64°, 21.14°, 23.44°, 24.35°, 24.66°, 25.80°, 26.42°, 26.82°, 27.37°, 28.30°, 28.85° and 29.65° allocated to the (*hkl*) crystal planes (−110), (020), (−104), (−202), (−122), (121), (−204), (104), (211), (114), (−222), (212), (−223), (−116), (131), (−224) and (−133), respectively, the characteristics arrangement of Cu(II) atom (JCPDS no. 23–1904). The standard JCPDS and observed 2θ data and *d*-spacing values are given in Table S2. The XRD pattern of the Ni (II) complex displays the peaks of 2θ scattering angles at 10.13°, 15.99°, 21.19°, 24.71°, 26.93°, 28.27°, 30.64°, 36.54°, 38.60° and 42.94° allocated to the (*hkl*) crystal planes (110), (113), (−115), (−116), (402), (−133), (420), (−228), (−336) and (−246), respectively, the characteristic well-ordered arrangement of Ni(II) atom (JCPDS no. 52–2481). The observed and standard JCPDS data for 2θ and *d*-spacing values are given in Table S3. The Co(II) complex exhibits peaks of 2θ scattering angles at 10.20°, 16.81°, 20.82°, 23.68°, 24.85°, 26.99°, 39.52° and 41.18° assigned to the (*hkl*) crystal planes (011), (112), (−311), (014), (−320), (023), (123), (306) and (117), respectively, the characteristics arrangement of Co(II) atom (JCPDS no. 72–1986). The standard JCPDS and observed data for 2θ and *d*-spacing values are given in Table S4. The Zn(II) complex shows peaks of 2θ scattering angles at 14.71°, 18.78°, 19.89°, 20.67°, 23.23°, 25.78°, 26.87°, 28.90°, 33.77° and 38.29° which are assigned to the (*hkl*) crystal planes (−101), (102), (112), (−111), (013), (200), (−201), (202), (−2–21), (214), (225) and (−3–23), respectively,

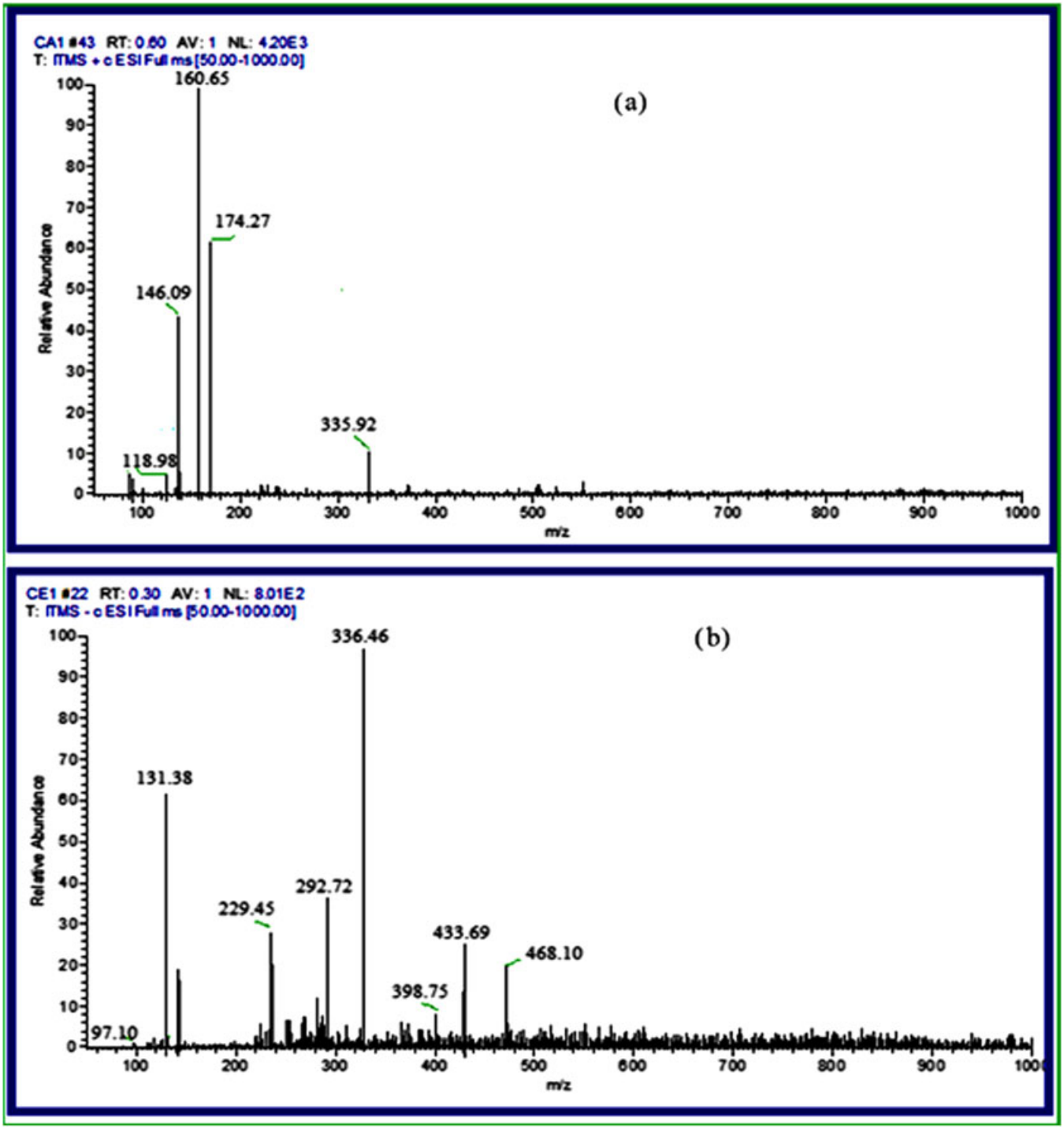

FIGURE 1 ESI-MS spectra of (a) Schiff base ligand and (b) Cu(II) complex

the characteristic well-ordered arrangement of Zn(II) atom (JCPDS no. 89–1341). The standard JCPDS and observed data for 2θ and *d*-spacing values are given in Table S5.

3.6 | EPR spectra

The EPR spectrum of the copper complex was recorded in the solid state at room temperature and is shown in Fig. S4 The spectrum exhibits axially symmetric *g*-tensor parameters with $g_{\parallel}$ (2.1552) > $g_{\perp}$ (2.0230) > 2.003 indicating that the copper site has a $dx^2 - y^2$ ground state attributed to square planar or octahedral stereochemistry.[32] A value of $g_{\parallel} > 2.3$ is characteristic of an ionic environment and $g_{\parallel} < 2.3$ indicates a covalent environment in metal–ligand bonding. The observed $g_{\parallel}$ values of complexes are less than 2.3 suggesting that the environment is covalent.[33]

In axial symmetry, the *g*-values are related by the expression

$$G = \left(g_{\parallel} - 2.0027\right)/\left(g_{\perp} - 2.0027\right) = 4$$

According to Hathaway and Billing,[34] for a value of G > 4, the exchange interaction between Cu(II) centres in the solid state is negligible, whereas if its value is <4, a considerable exchange interaction is indicated in the solid complex. The calculated *G* value for the copper complex is >4 suggesting that a copper–copper exchange interaction is negligible. The bonding parameters (α^2, β^2 and γ^2) of the Cu(II) complex have been calculated and are summarized in Table S6. These bonding parameters may be regarded as a measure of the covalency of the in-plane σ-bonds, in-plane π-bonds and out-of-plane π-bonds. Parameter α^2 can be calculated using the equation

$$\alpha^2 = \left(A_{\parallel}/P\right) + \left(g_{\parallel} - 2.0023\right) + 3/7\left(g_{\perp} - 2.0023\right) + 0.04$$

A value of $\alpha^2 = 0.5$ indicates pure covalent character whereas $\alpha^2 = 1.0$ denotes pure ionic character. In the present case, the value of α^2 (0.5966) of the $[CuLCl_2]$ complex indicates that the complex has some covalent character. The out-of-plane π-bonding (γ^2) and in-plane π-bonding (β^2) parameters have been calculated from the following expressions:

$$\beta^2 = \left(g_{\parallel} - 2.0023\right)E/\left(-8\lambda\alpha^2\right)$$
$$\gamma^2 = \left(g_{\perp} - 2.0023\right)E/\left(-2\lambda\alpha^2\right)$$

The observed β^2 (0.8320) and γ^2 (0.4932) values for $[CuLCl_2]$ indicate that there is interaction in the out-of-plane π-bonding whereas the in-plane π-bonding is completely ionic. This fact is confirmed by orbital reduction factors which are estimated using the following relations:

$$K_{\parallel}^2 = \left[\left(g_{\parallel} - 2.0023\right)\Delta E\right]/8\lambda_0$$
$$K_{\perp}^2 = \left[\left(g_{\perp} - 2.0023\right)\Delta E\right]/8\lambda_0$$

where λ_0 is the spin–orbit coupling constant for the Cu(II) ion ($-828\ cm^{-1}$) and $K_{\parallel}$ and $K_{\perp}$ are the parallel and perpendicular components of the orbital reduction factor (*K*). Significant information about the nature of bonding in the Cu(II) complex can be derived from the relative magnitudes of $K_{\parallel}$ and $K_{\perp}$. In the case of pure σ-bonding, $K_{\parallel} \approx K_{\perp}$; whereas $K_{\parallel} < K_{\perp}$ implies considerable in-plane π-bonding; while for out-of-plane π-bonding, $K_{\parallel} > K_{\perp}$. For the present case, the observed order is $K_{\parallel}$ (0.4890) > $K_{\perp}$ (0.2648) for $[CuLCl_2]$ implying a greater contribution from out-of-plane π-bonding than from in-plane π-bonding in metal–ligand π-bonding. The calculated f-factor ($g_{\parallel}/A_{\parallel}$) is considered as an empirical index of square planar distortion and is found to be 151, which is characteristic for slight to moderate distortion.[35]

3.7 | Binding studies

3.7.1 | Absorption titration

Absorption titration can be used to investigate the interaction of metal complexes with DNA. In general, if a complex binds to DNA through intercalation binding, usually the obtained results indicate hypochromism and red shift (bathochromism), due to the strong stalking interaction among the aromatic chromophore of the complex and the base pairs of DNA. The absorption spectra of the Cu(II) complex in the absence and presence of CT DNA are shown in Figure 2. The absorption spectra of copper, nickel, cobalt and zinc complexes show intense absorption bands at 352.2, 353.3, 351.7 and 354.1 nm, respectively, in 5 mM Tris–HCl/50 mM NaCl (pH = 7.2) buffer solution. Increasing the concentration of CT DNA resulted in a minor bathochromic shift in the range *ca* 2.8 to 2.2 nm and significant hypochromicity lying in the range *ca* 11 to 7% for all the complexes indicating appreciable intercalation binding of the complexes to CT DNA.[36]

The equilibrium binding constant values are 4.3×10^4, 3.9×10^4, 4.7×10^4 and $3.7 \times 10^4\ M^{-1}$ for copper(II), nickel(II), cobalt(II) and zinc(II) complexes. In order to compare the binding strength of the complexes with CT DNA, the intrinsic binding constants (K_b) are obtained by monitoring the changes in the absorbance for the complexes with increasing concentration of DNA. K_b is obtained from the ratio of slope to intercept of a plot of [DNA]/($\varepsilon_a - \varepsilon_f$) versus [DNA]. The K_b values are given in Table 1.

3.7.2 | Viscosity measurements

To further elucidate the interaction between the metal complexes and DNA, viscosity measurements were studied. A classic intercalative mode causes a considerable increase in viscosity of DNA solution due to the increase in overall DNA length. If the complexes bind completely in the DNA grooves by partial and/or non-classical intercalation under similar conditions, then this typically causes less pronounced (positive or negative) or no change in DNA solution viscosity. The effect of increasing the amount of metal complexes on the virtual viscosity of DNA is shown in Fig. S5 A gradual increase in virtual viscosity was observed on accumulation of the metal complexes to DNA solution suggesting essentially an intercalation mode of binding with the complexes,[37,38] i.e. the observed increase in the virtual viscosity of DNA could be the result of an increase in the duplex length on intercalation of the complexes. This observation may be elucidated by the insertion of the compounds in between the DNA base pairs, leading to an increase in the separation of base pairs at intercalation binding sites and, for that reason, an increase in overall DNA length.[39] The observed viscosity results are in accordance with absorption titration results.

3.7.3 | Fluorescence

In order to further investigate the interaction mode of the Schiff base metal complexes with DNA, a competitive binding experiment using EB as a probe was carried out. EB is a conjugate planar molecule with very weak fluorescence intensity due to fluorescence quenching of the free EB by

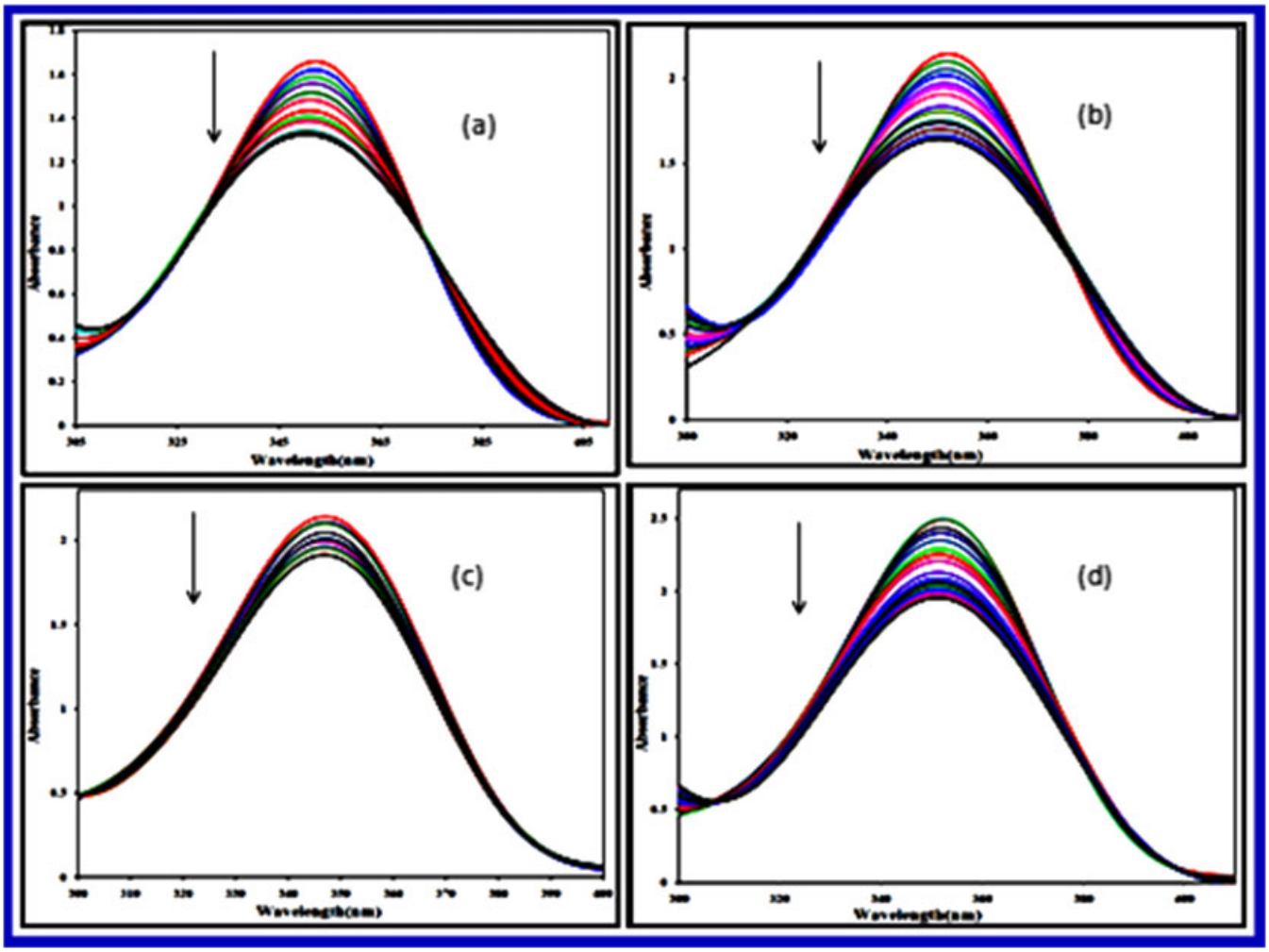

FIGURE 2 Absorption spectra of (a) $[CuLCl_2]$, (b) $[NiLCl_2]$, (c) $[CoLCl_2]$ and (d) $[ZnLCl_2]$ complexes in buffer (pH = 7.2) at 25°C in presence of increasing amounts of DNA. Arrow indicates the changes in absorbance with increasing DNA concentration

TABLE 1 Electronic absorption spectral properties of Cu(II), Ni(II), Co(II) and Zn(II) complexes with DNA

Compound	λ_{max} (nm)		$\Delta\lambda$ (nm)	H (%)[a]	K_b (M^{-1})[b]
	Free	Bound			
$[CuLCl_2]$	352.2	354.9	2.7	8.13	4.3×10^4
$[NiLCl_2]$	353.3	355.7	2.4	8.06	3.9×10^4
$[CoLCl_2]$	351.7	354.5	2.8	10.84	4.7×10^4
$[ZnLCl_2]$	354.1	356.3	2.2	7.89	3.7×10^4

[a]$H = [(A_{free} - A_{bound})/A_{free}] \times 100\%$.

[b]Intrinsic DNA binding constant determined from UV–visible absorption spectral titration.

solvent molecules, but it is greatly enhanced when EB is intercalated into the adjacent base pairs of double-stranded DNA. The enhanced fluorescence can be quenched upon the addition of a second molecule which could replace the bound EB or break the secondary structure of the DNA. On addition of metal complexes to CT DNA pretreated with EB ([DNA]/[EB] = 1) a significant reduction in the emission intensity (Figure 3) was observed, indicating the replacement of the EB fluorophore by the complexes, which results in a decrease of the binding constant of EB to DNA. As there was incomplete quenching of the EB-induced emission intensity, the intercalative binding mode was ruled out. The extent of quenching of the emission intensity gives a measure of the binding propensity of the interacting molecule with CT DNA. The Stern–Volmer quenching constant values, K_{SV}, obtained as the slope of I_0/I versus r ([complex]/[DNA]) have been evaluated for the Cu(II) and Co(II) complexes and found to be 2.11 and 2.32, respectively.

3.7.4 | Cyclic voltammetry

Cyclic voltammetric measurements of the Schiff base metal complexes were carried out. The cyclic voltammograms of the metal complexes in the absence and presence of varying amounts of DNA are shown in Figure 4. The incremental addition of CT DNA to the complexes causes a shift in the potential peak in cyclic voltammograms. This result shows that a complex stabilizes the duplex (GC pairs) by intercalating. Electrochemical parameters for the interaction of DNA with $[CuLCl_2]$, $[NiLCl_2]$, $[CoLCl_2]$ and $[ZnLCl_2]$ metal(II) complexes are summarized in Table 2. The Ip_c/Ip_a ratios of these four redox couples of the complexes are 0.7132, 0.5682, 0.6143 and 0.6415, respectively, which indicate that

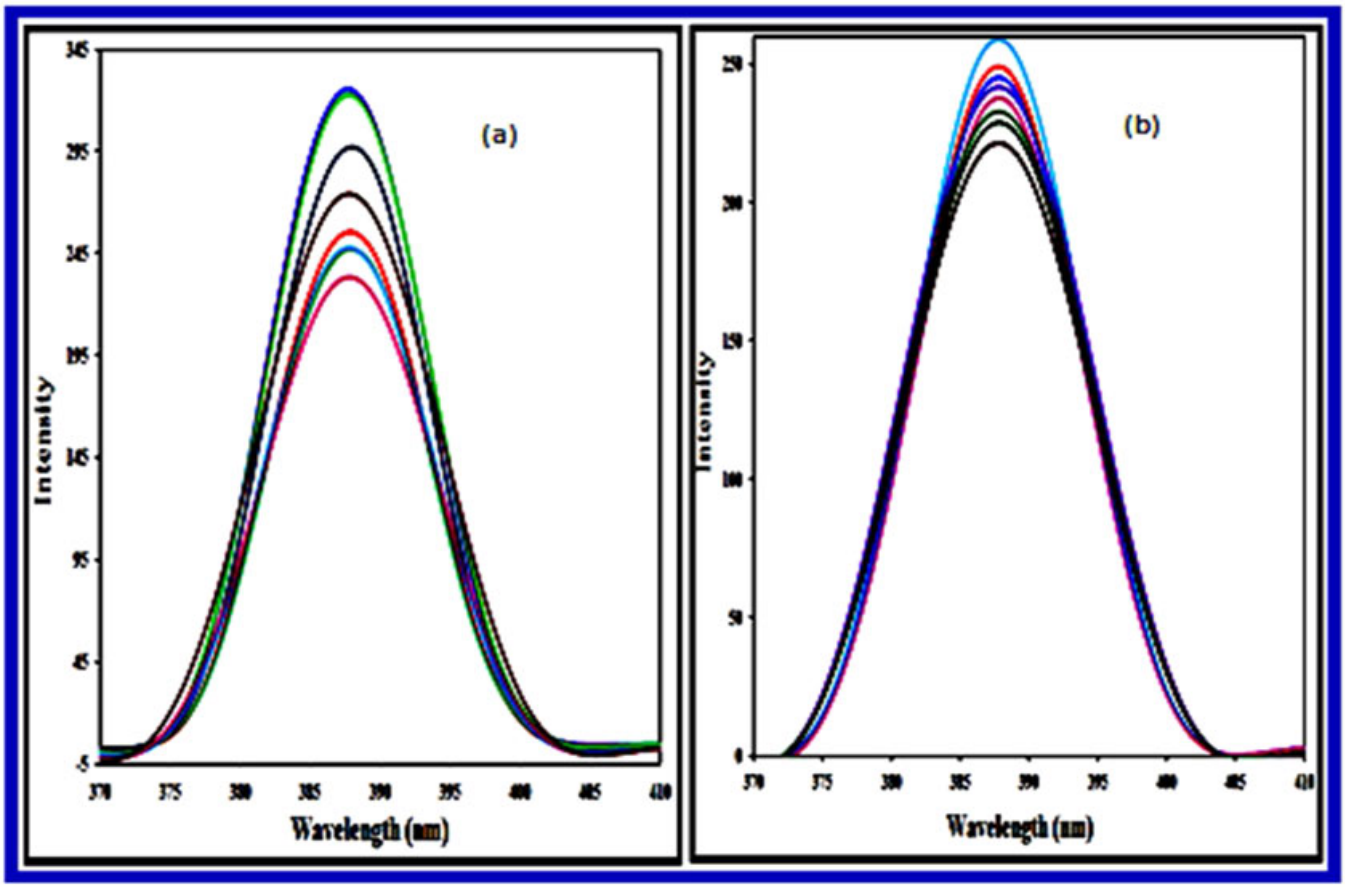

FIGURE 3 Emission spectra of $[CuLCl_2]$ and $[CoLCl_2]$ complexes in buffer (pH = 7.2) at 25°C in presence of increasing amounts of DNA

the reaction of the complexes on the glassy carbon electrode surface is a quasi-reversible redox process. The ratio of Ip_a/Ip_c is approximately unity. This indicates the quasi-reversible redox process of the metal complexes. During the incremental addition of CT DNA to the complexes the redox couples caused a negative shift in $E_{1/2}$ and a decrease in ΔEp. Addition of CT DNA to the complexes causes a positive shift in the potential and a decrease in the current intensity. From these data, it is understood that all the synthesized complexes interact with DNA in an intercalating manner.[40]

In addition, in differential pulse voltammograms of $[MLCl_2]$ in the absence and presence of varying amounts of DNA with significant decrease of current intensity (Figure 5), the shift in potential is related to the ratio of binding constants by the following equation:

$$E_b - E_f = 0.0591 \times \log\left(K_{[red]}/K_{[ox]}\right)$$

where E_b and E_f are peak potentials of the complex in bound and free forms, respectively. The present Schiff base complexes show one-electron transfer during the redox process and the Ip_a/Ip_c value is less than unity which indicates the reaction of the complexes on the glassy carbon electrode surface is quasi-reversible. Other complexes (Co(II), Ni(II) and Zn(II)) show considerable shift in both cathodic and anodic peak potentials in the presence of incremental addition of CT DNA. Most of the synthesized complexes show both anodic and cathodic peak potential shifts which are either positive or negative (Table 2). This indicates the intercalating mode of DNA binding with the Schiff base complexes.

3.8 | DNA cleavage activity

The cleavage reaction was screened by gel electrophoresis. The electrophoresis obviously indicated that the Schiff base L and its metal(II) complexes have interacted with DNA as there was a difference in the bands of lanes 1–5 compared to the control DNA (Figure 6). The Schiff base metal complexes are able to convert supercoiled DNA into open circular DNA. In general, oxidative mechanisms account for DNA cleavage by hydroxyl radicals via abstraction of a hydrogen from sugar units and predict the release of specific residues arising from transformed sugars, depending on the position from which the hydrogen is removed.[41] The reaction is modulated by a bound hydroxyl radical or a peroxo species generated from H_2O_2. In this study, the pUC19 DNA gel electrophoresis experiment was conducted at 35°C using the synthesized complexes in the presence of H_2O_2 as oxidant. From Figure 6, it is observed that the control DNA (lane 1) does not show any significant cleavage of pUC19 DNA even

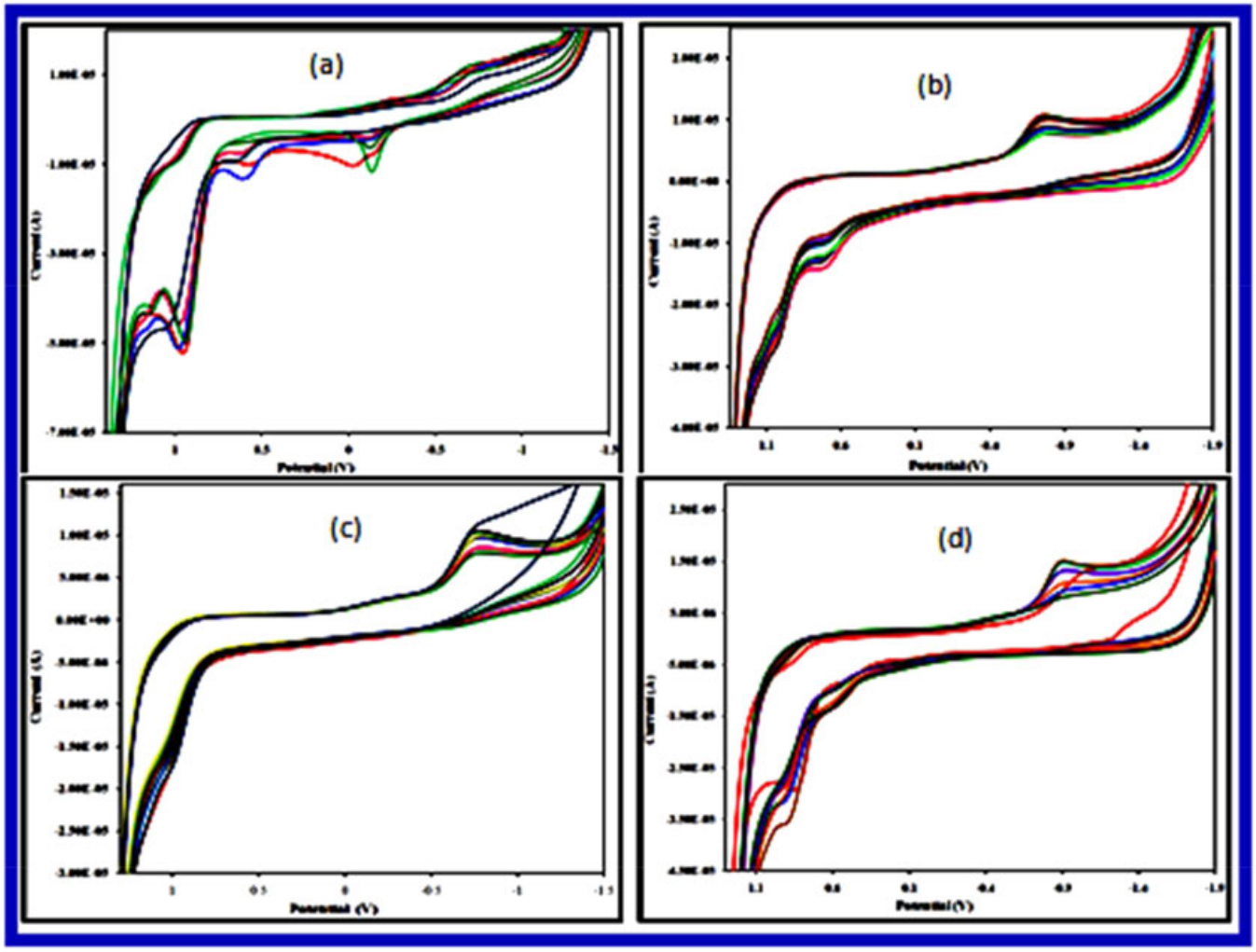

FIGURE 4 Cyclic voltammograms of (a) [$CuLCl_2$], (b) [$NiLCl_2$], (c) [$CoLCl_2$] and (d) [$ZnLCl_2$] complexes in buffer (pH = 7.2) at 25°C in presence of increasing amounts of DNA

TABLE 2 Electrochemical parameters for interaction of DNA with Cu(II), Ni(II), Co(II) and Zn(II) complexes

Compound	$E_{1/2}$ (V)[a]		ΔEp (V)[a]		Ip_a/Ip_c[b]
	Free	Bound	Free	Bound	
[$CuLCl_2$]	0.112	0.134	−1.646	−1.615	0.7132
[$NiLCl_2$]	0.007	0.021	−1.448	−1.42	0.5682
[$CoLCl_2$]	0.125	0.141	−1.681	−1.676	0.6143
[$ZnLCl_2$]	0.003	0.009	−1.719	−1.769	0.6415

[a]Data from cyclic voltammetric measurements. $E_{1/2}$ is calculated as the average of anodic (Ep_a) and cathodic (Ep_c) peak potentials: $E_{1/2} = (Ep_a + Ep_c)/2$; $\Delta Ep = Ep_a - Ep_c$.

[b]Error limit: ±5%.

for longer exposure time. Co(II) and Cu(II) complexes (lanes 4 and 5) cleave DNA as compared to control DNA while the other complexes do moderately cleave in the presence of H_2O_2. The results indicate the presence of radical cleavage[42] and the cleavage efficiency of the complexes is comparable to the control, due to their efficient DNA-binding ability. As the compounds were observed to cleave DNA, it is concluded that the compounds inhibit the growth of pathogenic organisms by cleaving the genome.

3.9 | Molecular docking with DNA

The docking of the Schiff base ligand complexes with DNA was performed to rationalize the results of DNA binding study. The best docked poses are shown in Figure 7. It is obvious that the metal complexes get attached to DNA through intercalation binding mode between the nucleotide base pairs of DNA. Energetically favourable docked poses were obtained from the rigid molecular docking experiments agreeing between the optimized energy-minimized structures (Figure 7) for the ligand and Cu(II), Ni(II), Co(II) and Zn(II) complexes with DNA duplex of sequence d $(CGCGAATTCGCG)_2$ dodecamer (PDB ID: 1BNA). On analysing the docked structures, it is evident that the metal complexes fit well into the A-T rich region of target DNA. The Schiff base and its metal complexes are stabilized in the A-T rich region through various interactions, such as

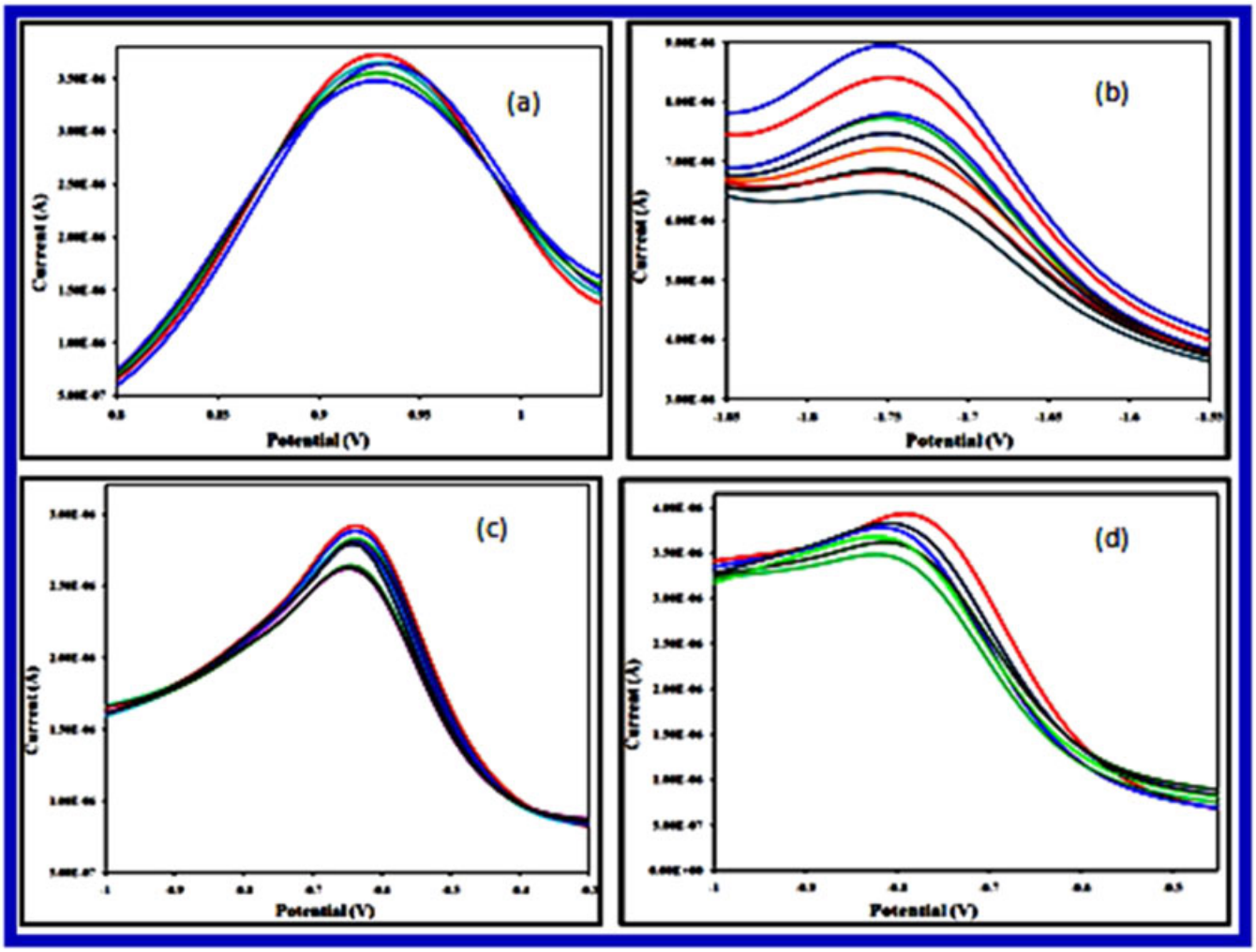

FIGURE 5 Differential pulse voltammograms of (a) $[CuLCl_2]$, (b) $[NiLCl_2]$, (c) $[CoLCl_2]$ and (d) $[ZnLCl_2]$ complexes in buffer (pH = 7.2) at 25°C in the presence of increasing amounts of DNA

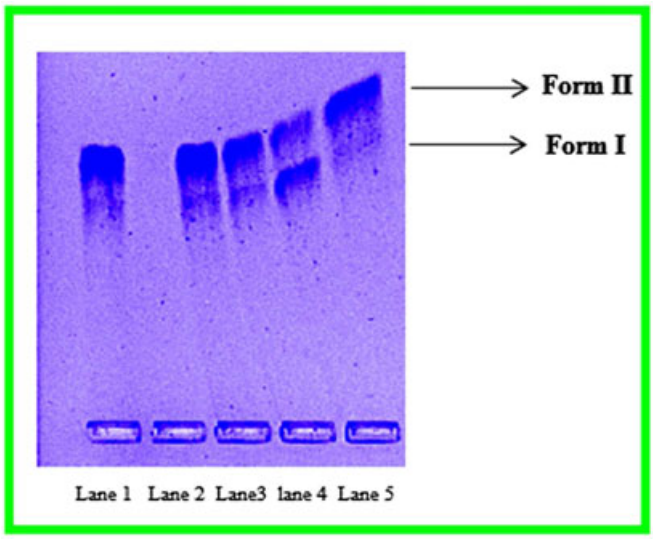

FIGURE 6 Gel electrophoretic separation of plasmid pUC19 DNA treated with $[MLCl_2]$ complexes. Lane 1: DNA + ligand + H_2O_2; Lane 2: DNA + $[ZnLCl_2]$ + H_2O_2; Lane 3: DNA + $[NiLCl_2]$ + H_2O_2; Lane 4: DNA + $[CoLCl_2]$ + H_2O_2; Lane 5: DNA + $[CuLCl_2]$ + H_2O_2

van der Waals and hydrophobic interactions.[43] The Schiff base ligand and its Cu(II), Ni(II), Co(II) and Zn(II) metal complexes have docking scores of −212.34, −225.57, −224.18, −225.20 and −223.95, respectively. A compound with a higher negative docking score is deemed as more potent. In the present study, Cu(II) and Co(II) complexes have higher docking scores and hence they have more activity. Minimum activity is found for the Schiff base ligand as it has a low docking score of −212.34.

3.10 | Antimicrobial activity

Antibacterial activity of the Schiff base ligand and its metal complexes was determined using the paper disc method. The Schiff base ligand and its complexes were screened against four bacterial strains, *K. pneumoniae*, *B. subtilis*, *E. coli* and *S. typhi*, and the fungi *A. flavus*, *A. niger* and *C. albicans*. The results presented in Table 3 reveal that Schiff base ligand and its complexes have some activity, but they are not as active as the standard drugs (ampicillin for bacteria

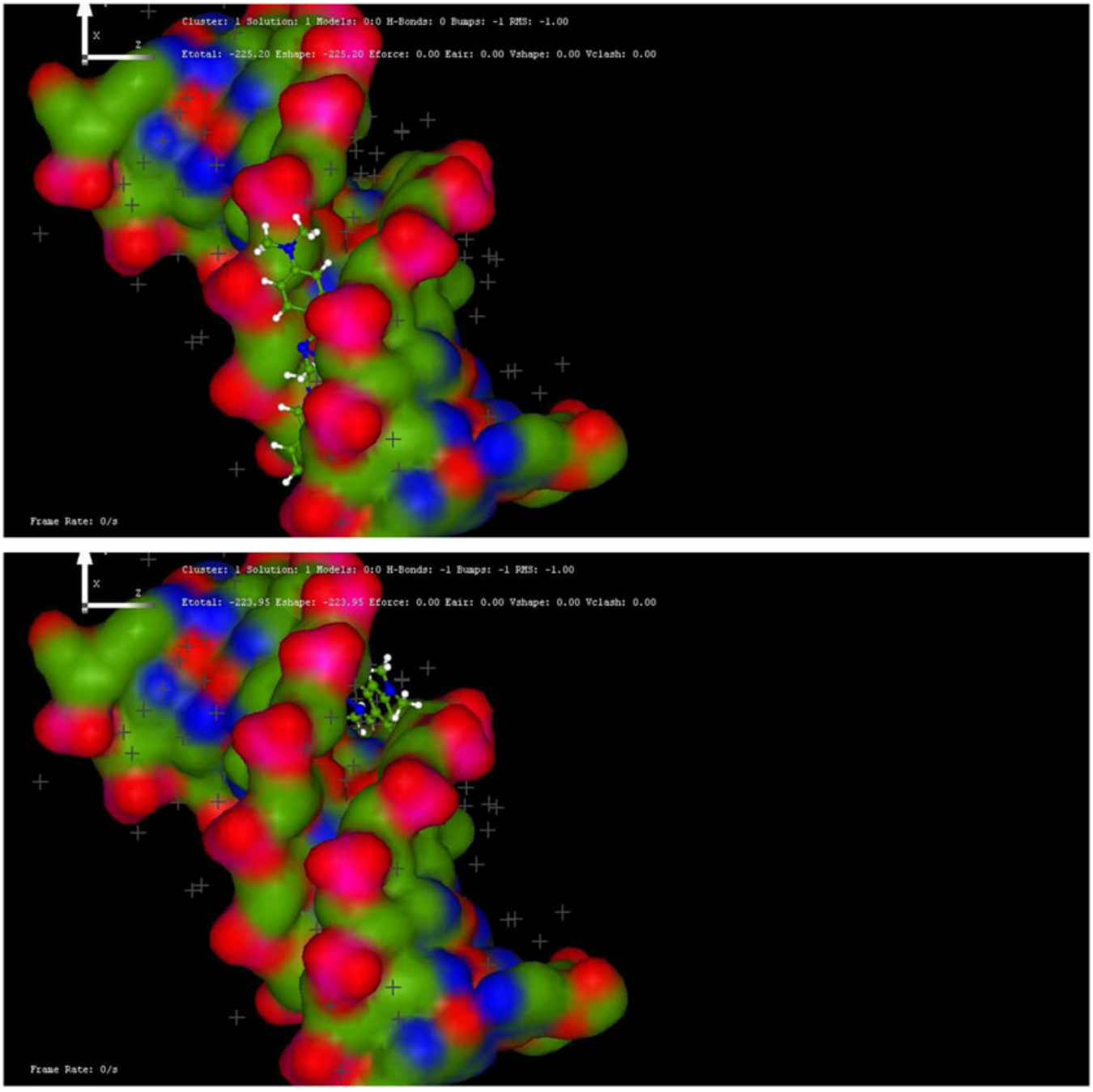

FIGURE 7 Interaction of the complexes [$NiLCl_2$] and [$ZnLCl_2$] with d(CGCGAATTCGCG) strands of DNA

TABLE 3 *In vitro* antimicrobial activity of Schiff base and its metal complexes (zone of inhibition in mm)

Compound	Bacteria				Fungi		
	E. coli	*B. subtilis*	*K. pneumoniae*	*S. typhi*	*A. flavus*	*C. albicans*	*A. niger*
L	8	10	13	11	19	15	18
[$CuLCl_2$]	21	20	23	21	27	19	26
[$NiLCl_2$]	19	22	16	15	20	24	21
[$CoLCl_2$]	20	17	21	23	24	20	27
[$ZnLCl_2$]	17	21	15	17	19	22	22
Ampicillin[a]	26	29	24	22	—	—	—
Ciprofloxacin[b]	—	—	—		35	30	35

[a]Ampicillin was used as the standard for bacteria.

[b]Ciprofloxacin is used as the standard for fungi.

and ciprofloxacin for fungi). However, the results reveal that the metal complexes have a higher inhibitory activity than the Schiff base ligand against both Gram-positive and Gram-negative bacteria.

The metal complexes show better antimicrobial activity than the ligand. According to the Overtone concept of cell permeability, the lipid membrane surrounding a cell favours the passage of only lipid-soluble materials, and therefore liposolubility is an important factor which controls antimicrobial activity. On chelation, the polarity of the metal ion is reduced to a greater extent due the overlapping of the ligand orbital and partial sharing of the positive charge of the metal ion with donor groups. The resulting increased lipophilicity enhances the penetration of the complexes into the lipid membranes and blocks the metal binding sites in the enzymes of the microorganisms. These complexes also disturb the respiration process of cells and thus block the synthesis of proteins, which restricts further growth of the organism.[44]

4 | CONCLUSIONS

In this study, a biologically significant Schiff base ligand and its Cu(II), Ni(II), Co(II) and Zn(II) metal complexes have been synthesized and characterized. The physicochemical and spectral data reveal that all the complexes are mononuclear and adopt square planar geometry around the metal ion. The Schiff base complexes bind to CT DNA and such binding ability has been explored using diverse techniques. The data obtained prove that the complexes act as efficient metallointercalators. The agarose gel electrophoresis studies show that the complexes can promote the oxidative cleavage of plasmid DNA. However, these observations and a more extensive study would be necessary in order to assert that the complexes act as cleavage agents. The docked structures reveal that the complexes can fit well with intercalative binding of DNA with a binding site of three base pairs preferably involving the A-T residues. The biological data indicate that the complexes have higher antimicrobial activity than the free Schiff base ligand. The cooperative biological activities of the complexes may be helpful for the design of metal-based drugs.

ACKNOWLEDGEMENTS

The authors express their heartfelt thanks to the College Managing Board, Principal and Head of the Department of Chemistry, VHNSN College for providing necessary research facilities. IIT Bombay and CDRI, Lucknow, are gratefully acknowledged for providing instrumental facilities.

REFERENCES

[1] N. Charef, F. Sebti, L. Arrar, M. Djarmouni, N. Boussoualim, A. Baghiani, S. Khennouf, A. Ourari, M. A. Al Damen, M. S. Mubarak, D. G. Peters, *Polyhedron* **2015**, *85*, 450.

[2] A. Gulcu, M. Tumer, H. Demirelli, R. A. Wheatley, *Inorg. Chim. Acta* **2005**, *358*, 1785.

[3] X. Zhou, L. Shao, Z. Jin, J. B. Liu, H. Dai, J. X. Fang, *Heteroatom Chem.* **2007**, *18*, 55.

[4] I. J. Patel, S. J. Parmar, *E-J. Chem.* **2010**, *7*, 617.

[5] K. M. Khan, M. Khan, M. Ali, M. Taha, S. Rasheed, S. Perveen, M. I. Choudhary, *Bioorg. Med. Chem.* **2009**, *17*, 7795.

[6] O. A. E. Gammal, *Inorg. Chim. Acta* **2015**, *435*, 73.

[7] E. Akila, M. Usharani, R. Rajavel, *Int. J. Pharm. Pharm. Sci.* **2013**, 5,573.

[8] A. E. Motaleb, M. Ramadan, M. Ibrahim, Y. Shaban, *J. Mol. Struct.* **2011**, *1006*, 348.

[9] P. Viswanathamurthi, K. Natarajan, *Synth. React. Inorg. Met.-Org. Chem.* **2006**, *36*, 415.

[10] H. Keypour, A. Shooshtari, M. Rezaeivala, F. O. Kup, H. A. Rudbari, *Polyhedron* **2015**, *97*, 75.

[11] M. M. Ali, M. Jesmin, M. K. Sarker, M. S. Salahuddin, M. R. Habib, J. A. Khanam, *Int. J. Biol. Chem. Sci.* **2008**, *2*, 292.

[12] M. T. Behnamfar, H. Hadadzadeh, J. Simpson, F. Darabi, A. Shahpiri, T. Khayamian, M. Ebrahimi, H. A. Rudbari, M. Salimi, *Spectrochim. Acta A* **2015**, *134*, 502.

[13] N. Shahabadi, S. Kashanian, F. Darabi, *Eur. J. Med. Chem.* **2010**, *45*, 4239.

[14] L. Leelavathy, S. Anbu, M. Kandaswamy, N. Karthikeyan, N. Mohan, *Polyhedron* **2009**, *28*, 903.

[15] M. Gaber, H. A. E. Ghamry, S. K. Fathalla, *Spectrochim. Acta A* **2015**, *139*, 396.

[16] J. Hong, Y. Jiao, J. Yan, W. He, Z. Guo, L. Zhu, J. Zhang, *Inorg. Chim. Acta* **2010**, *363*, 793.

[17] V. da Silveira, H. Benezra, J. Luz, R. Georg, C. Oliveira, A. Ferreira, *J. Inorg. Biochem.* **2011**, *105*, 1692.

[18] N. Raman, R. Mahalakshmi, L. Mitu, *Spectrochim. Acta A* **2014**, *131*, 355.

[19] W. Song, J. Cheng, D. Jiang, L. Guo, M. Cai, H. Yang, Q. Lin, *Spectrochim. Acta A* **2014**, *121*, 70.

[20] P. Kavitha, M. Saritha, K. Reddy, *Spectrochim. Acta A* **2013**, *102*, 159.

[21] G. Li, K. Du, J. Wang, J. Liang, J. Kou, X. Hou, L. Ji, H. Chao, *J. Inorg. Biochem.* **2013**, *119*, 43.

[22] M. Shebl, *Spectrochim. Acta A* **2014**, *117*, 127.

[23] M. Saif, M. M. Mashaly, M. F. Eid, R. Fouad, *Spectrochim. Acta A* **2012**, *92*, 347.

[24] X. J. Tan, H. Z. Liu, C. Z. Ye, J. F. Lou, Y. Liu, D. X. Xing, S. P. Li, S. L. Liu, L. Z. Song, *Polyhedron* **2014**, *71*, 119.

[25] G. H. Wolfe, G. H. Shimer, S. T. Meehan, *Biochemistry* **1987**, *26*, 6392.

[26] M. I. Rahman, W. J. Choudhary, *Bioassay Techniques for Drug Development*, Harwood Academic, Amsterdam **2001** 16.

[27] C. Muthukumar, A. Sabastiyan, M. Ramesh, M. Subramanian, M. Y. Suvaikin, *Int. J. ChemTech Res.* **2012**, *4*, 1322.

[28] K. Nakamato, *Infrared and Raman Spectra of Inorganic and Coordination Compounds*, Wiley, New York, **1971**.

[29] P. F. Rapheal, E. Manoj, M. R. P. Kurup, *Polyhedron* **2007**, *26*, 818.

[30] R. Kannappan, S. Tanase, I. Mutikainen, U. Turpeinen, J. Reedijk, *Inorg. Chim. Acta* **2005**, *358*, 383.

[31] D. Sakthilatha, R. Rajavel, *Chem. Sci. Trans.* **2013**, *2*, 711.

[32] F. E. Mabbs, D. Collison, *Electron Paramagnetic Resonance of Transition Metal Compounds*, Elsevier, Amsterdam, **1992**.

[33] B. J. Hathaway, in *Comprehensive Coordination Chemistry*, Vol. 5 (Eds: G. Wilkinson, R. D. Gillard, J. A. McCleverty), Pergamon Press, Oxford, **1987**, p. 534.

[34] B. J. Hathaway, D. E. Billing, *Coord. Chem. Rev.* **1970**, *5*, 143.

[35] M. Choudhary, R. N. Patel, S. P. Rawat, *J. Mol. Struct.* **2014**, *1070*, 94.

[36] M. Iqbal, S. Ali, M. Nawaz Tahir, N. Muhammad, N. A. Shah, M. R. Sohail, V. Pandarinathan, *J. Mol. Struct.* **2015**, *1093*, 135.

[37] S. Sathyanarayana, J. Dabroniak, J. Chaires, *Biochemistry* **1992**, *31*, 9319.

[38] L. Jin, P. Yang, *J. Inorg. Biochem.* **1997**, *68*, 79.

[39] M. Patel, H. Josh, C. Patel, *Spectrochim. Acta A* **2013**, *104*, 48.

[40] G. Pratviel, J. Bernadou, B. Meunier, *Adv. Inorg. Chem.* **1998**, *45*, 251.

[41] K. Fukui, *Science* **1982**, *218*, 747.

[42] N. Raman, A. Kulandaisamy, A. Shanmugasudaram, *Transition Met. Chem.* **2001**, *26*, 131.

[43] P. Arthi, S. Shobana, P. Srinivasan, L. Mitu, A. K. Rahiman, *Spectrochim. Acta A* **2015**, *143*, 49.

[44] Y. Anjaneyulu, R. P. Rao, *Synth. React. Inorg. Org. Chem.* **1986**, *16*, 257.

SUPPORTING INFORMATION

Additional supporting information can be found in the online version of this article at the publisher's website.

How to cite this article: Packianathan, S., Kumaravel, G., and Raman, N. (2016), DNA interaction, antimicrobial and molecular docking studies of biologically interesting Schiff base complexes incorporating 4-formyl-*N*,*N*-dimethylaniline and propylenediamine, *Appl. Organometal. Chem.*, doi: 10.1002/aoc.3577